2R.3 MICROPHYSICAL AND KINEMATIC STRUCTURES WITHIN DRIZZLING STRATOCUMULUS IN THE SOUTHEAST PACIFIC

Kimberly Comstock[1] *, Sandra Yuter[2], and Robert Wood[1]
1. University of Washington, Seattle, Washington
2. North Carolina State University, Raleigh, North Carolina

1. INTRODUCTION

Vast regions of subtropical stratocumulus (Sc) clouds are a significant source of cooling in the earth's radiation budget. Southeast Pacific Sc also play a supporting role in the seasonal cycle of the East Pacific Ocean and the El Niño-Southern Oscillation. Drizzle from the Sc can affect the boundary layer dynamics and therefore the radiative properties of the cloud layer. Unfortunately, these clouds have proven difficult for climate models to simulate.

Observations obtained during the 2001 East Pacific Investigation of Climate stratocumulus study (EPIC Sc, Bretherton et al., 2004) were designed to provide insight into the physical processes of drizzling Sc with an eventual goal of improving model parameterizations. The unique EPIC data set includes high temporal and spatial resolution observations of clouds and drizzle from a vertically-pointing millimeter cloud radar (MMCR) and a scanning C-band radar.

Open cellular cloud patterns in Sc consist of clear regions surrounded by 'rings' of clouds. Conversely, the closed-cellular regime consists of cloudy regions surrounded by clear air (e.g. Agee et al., 1973). While the closed cellular regime is most typical in the southeast Pacific, open-cellular regions are not uncommon. Wood and Hartmann (2005) found that during Sept-Oct 2000, closed cells occurred up to 70% of the time near the west coast of South America, and open cellular structures were common up to 50% of the time farther off shore. Recent findings suggest that during the EPIC Sc study, open-cellular convection was more frequently associated with higher rain rates than closed-cellular convection (Stevens et al., 2005; Yuter and Comstock, 2005).

Comstock et al. (2005) developed a conceptual model for the drizzling Sc boundary layer associated with open cellular regions embedded within closed-cellular Sc. We use high resolution reflectivity and radial velocity data from the C-band radar's RHI scans to develop a more detailed picture of the vertical structure of drizzle cells. We analyze cases from each regime separately to determine whether different dynamics are at play in drizzling open vs. closed cellular convection.

2. DATA

All data used in this analysis are from the on-station period of EPIC Sc (16-22 October 2001), when the NOAA research vessel Ronald H. Brown was located at 20°S, 85°W near the center of the southeast Pacific Sc region (Bretherton et al., 2004). Open and closed cellular scenes were classified by eye using GOES satellite images, as described in Yuter and Comstock (2005). Within these categorized times, we selected a subset of data to analyze more closely, including 13 hours of open-cellular and 6 hours of closed-cellular data that contained sufficient C-band radar echo.

During EPIC Sc, the vertically-pointing, 8.6 mm wavelength NOAA Environmental Technology Laboratory MMCR obtained a 90 m vertical-resolution reflectivity profile every 10 seconds (Moran et al., 1998). In heavy drizzle, the MMCR occasionally saturated below or even within the cloud layer (Comstock et al., 2004). The MMCR was not stabilized on the ship, so the radial velocity information could not be used.

The shipboard 5-cm wavelength scanning C-band radar is sensitive to drizzle and heavier precipitation but not clouds (Ryan et al., 2002). The C-band minimum-detectable reflectivity was about -12 dBZ at 30 km. The scan strategy, described in Appendix A of Comstock et al. (2004), included one 30-km radius volume scan every five minutes and a set of four RHI scans (north, south, east and west) every five minutes, but only 10 times an hour.

The MMCR-derived cloud-top height was used to vertically normalize the RHI data. This was done to smooth out antenna pointing-angle inaccuracies and to ensure consistency in cloud top height between RHIs obtained at the same time. The data were then interpolated to 75 m horizontal and 100 m vertical resolution. A 500 m horizontal-resolution

* *Corresponding author address*: Department of Atmospheric Sciences, University of Washington, Box 351640, Seattle, WA 98195; *e-mail*: kcomstock@atmos.washington.edu, web site: http//www.atmos.washington.edu/∼kcomstock/papers.html

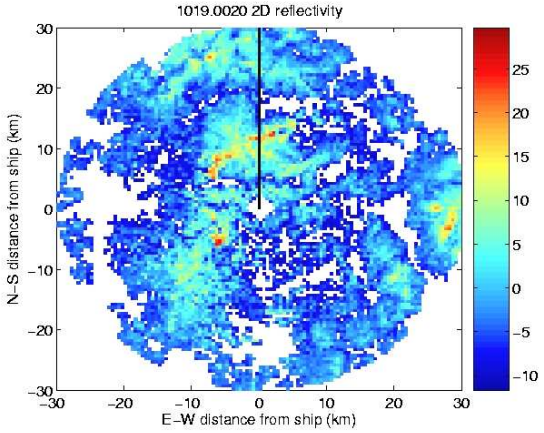

Figure 1: 2D reflectivity map at 0020 UTC on 19 October 2001. Black line corresponds to 0°RHI shown in Fig. 2.

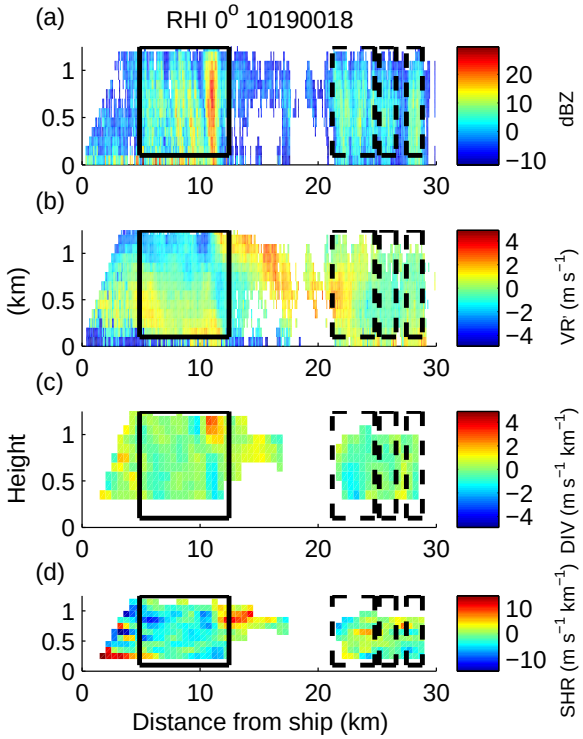

Figure 2: RHI at 0°at 0018 UTC 19 October 2001. (a) reflectivity, (b) radial velocity minus the mean, (c) divergence, and (d) shear. Black solid box corresponds to high-reflectivity drizzle cell mask, and dashed boxes are for moderate-reflectivity cell masks. In the radial velocity panel, positive velocity indicates flow away from the radar, located at 0 km.

radial velocity (VR) data set, filtered using a 1-2-1 filter, was used to compute the radial component of divergence (DIV) and shear (SHR). In this paper, DIV and SHR will always refer to the radial components. The large number of RHIs in four directions through randomly-oriented drizzle cells justifies our assumption that the results are not biased by the restriction of the data to the radial direction. The 3D volume scans were vertically interpolated (between 500 m and 2 km) into 2D maps with 500 m horizontal resolution to mitigate the impact of antenna pointing angle uncertainties.

3. METHOD

Reflectivity (Z) values within each RHI scan were subdivided into three categories in addition to the 'all' Z category. Contiguous regions of drizzle with $Z \geq 5$ dBZ (equivalent to a cloud base rain rate of about 5 mm day^{-1}, Comstock et al., 2004) were identified as 'moderate' Z drizzle cells. If these regions had a peak $Z \geq 15$ dBZ (about 29 mm day^{-1}), they were instead categorized as 'high' Z drizzle cells. All remaining regions not assigned to moderate or high-Z drizzle, where $Z < 5$ dBZ, were categorized as 'no cell.' Data within each of these categories were analyzed by computing contoured frequency-by-altitude diagrams (CFADs, Yuter and Houze, 1995), or joint frequency distributions of Z, VR, DIV and SHR, at each altitude where data were available.

Figure 1 shows 2D vertically averaged Z from the C-band radar obtained at 0020 UTC on 19 October 2001. The 0°RHI is marked. Four cross sections derived from this RHI are shown in Fig. 2: Z, VR minus the mean VR, DIV, and SHR. The box outlined by solid black lines corresponds to the high-Z drizzle mask. The high-Z drizzle cell in this example includes a 8 km wide region of $Z > 5$ dBZ where the peak Z values are offset from the center of the box. Boxes outlined with dashed lines correspond to the moderate-Z drizzle mask. The no-cell Z category includes all reflectivity (and corresponding VR, SHR and DIV) outside of the boxes. The 'all' category corresponds to all detectable signal shown.

4. RESULTS

The radial velocity associated with the high-Z drizzle cell in Fig. 2b shows converging flow (in the radial direction) below about 700-800 meters and diverging flow above. The inflow and outflow regions are at least 10 km wide and continue outside what we have defined as the boundary of the cell. The computed divergence signal depicted in Fig. 2c is much narrower, peaking where reflectivity is strongest between about 10 and 12 km from the ship.

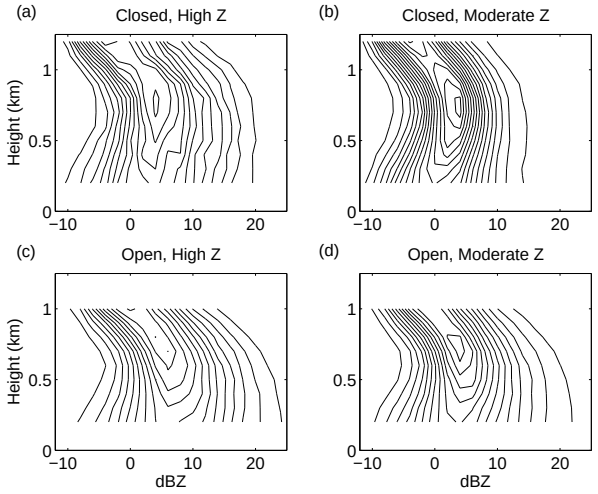

Figure 3: CFADs of reflectivity for RHIs. (a) Closed-cellular regime, high-reflectivity drizzle, (b) Closed-cellular regime, moderate-reflectivity drizzle, (c) Open-cellular regime, high-reflectivity drizzle, and (d) Open-cellular regime, moderate-reflectivity drizzle. Contour interval is 0.05.

Within individual RHIs, regions of convergence and divergence were observed with horizontal scales of about 2-15 km (approx 20 samples of each), with the mode between 5 and 8 km. These scales may be underestimated because the C-band radar can only capture the radial velocity where there are sufficient scatterers (drizzle), and only within 30 km of the radar. Regions of sub-cloud inflow to and cloud-top outflow from the cell are observed to be 10-20 km in scale horizontally (9 examples), showing that the drizzle cells are associated with mesoscale circulations.

High-Z drizzle cells made up a higher percentage of the drizzle cells in the open regime than the closed-cellular regime during the EPIC Sc on-station period (see Table 1). Moderate-Z cells were more common during the closed-cellular drizzling period. The values in Table 1 are dependent on the threshold values chosen for the drizzle cells (i.e. 5 and 15 dBZ), but the given percentages are consistent within about 10-15% for a reasonable range of thresholds.

Increasing Z with decreasing height in the mode of the CFADS in Fig. 3 indicates precipitation particle growth from the top of the cloud to just below cloud base. Decreasing Z below cloud base (600-900 m) indicates below-cloud evaporation, particularly in the moderate-Z cells. The CFADs show that in open-cellular conditions higher Z values are more common and more drizzle reaches the surface (less evaporates). For both open and closed cellular regimes, high-Z drizzle cells exhibit a wider distribution of Z values at a given altitude, indicating that high-Z drizzle cells are more heterogeneous than moderate-Z cells.

Table 1: Total number of drizzle cells and distribution among drizzle categories (%) for each cloud regime. There were 6 hours of closed-cellular and 13 hours of open-cellular data.

	Cloud regime	
Drizzle category	Closed	Open
High Z	120 (10%)	283 (28%)
Moderate Z	1122 (90%)	744 (72%)

On the $\sim$1 km scale, there is a broad range of convergence and divergence associated with drizzle cells in both closed and open regimes. Drizzle cells contain both converging and diverging kinematic patterns. To isolate the convergence and divergence in the core of the drizzle cells where Z tends to be highest, we compute the CFADs of divergence *only where the Z is greater than the mean Z at each height*.

Figure 4 shows these CFADs, and Fig. 5a and b show the mean and median profiles of conditional Z normalized by the average cloud top height for each regime. The CFADs in Fig. 4 provide evidence of convergence at low to mid levels (about 200-700 m) and divergence within the cloud layer (about 800-1200 m) for drizzle-cell cores. The divergence distributions in Fig. 4 are not vertically symmetric, which suggests stronger cloud-top outflow and subsiding air outside of the observable drizzle cells. This is also illustrated by the mean and median profiles of divergence in Fig. 5c and d, which pertain to the entire drizzle cells and not just the cores.

As apparent in Figs. 3 and 4, the cloud top is higher for the closed cellular times (1.4 km as opposed to 1.2 km for the open times). Some of the difference in cloud top height can be explained by the diurnal cycle of cloud top. All of the closed-cellular samples were obtained during the night or early morning hours when the cloud top tended to be highest (Bretherton et al., 2004), while about 30% of the open-cellular cases were from the afternoon or evening when cloud top was typically lowest. Lower cloud tops during open-cellular periods are consistent with decreased entrainment rates. Entrainment is largely driven by cloud-top radiative cooling, which would be less for the lower cloud fraction of the open-cellular regime.

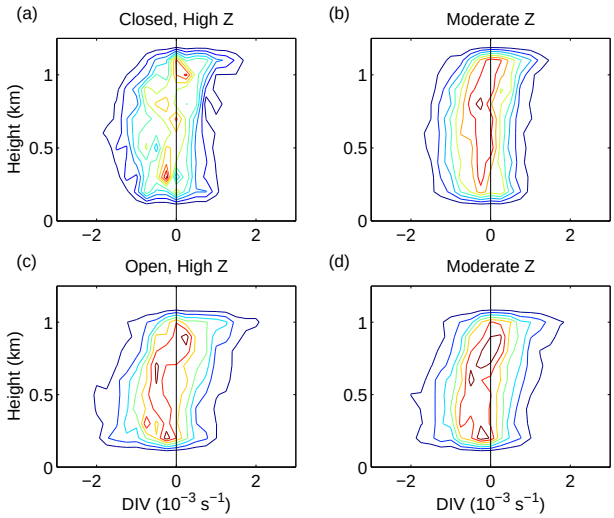

Figure 4: As in Fig. 3, but CFADs of divergence for RHIs *only where reflectivity is greater than the mean*. The number of samples in each subcategory is provided in Table 1. Contour interval is 0.02.

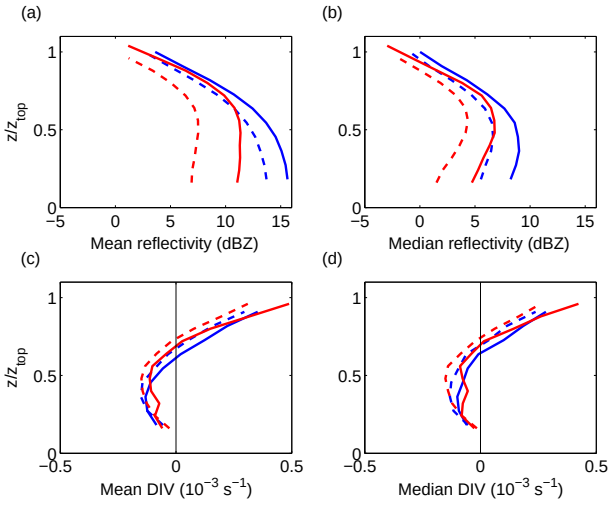

Figure 5: (a) Mean and (b) median conditional reflectivity profiles, (c) mean and (d) median divergence profiles plotted normalized by average cloud top height (z_{top}) for each regime. Profiles correspond to high (solid) and moderate (dashed) reflectivity drizzle cells during open (blue) and closed (red) cellular cloud regimes. The modes are nearly identical to the median profiles.

Figure 2d shows a shear layer between about 12 and 15 km from the ship, extending about 4 km beyond the cell. This common drizzle-cell feature is caused by outflow near cloud top overlying subcloud inflow. Divergence overlying convergence in a drizzle cell was observed in individual RHIs to cause the strongest shear layers. However, this signal tends to yield opposite signs of shear on either side of the cell. The background shear varied from case to case, but was, on average, slightly positive in the lower half of the boundary layer, and close to zero or slightly negative in the cloud layer. Because it was similar in both regimes, we expect the background shear is not a factor in determining open vs. closed-cellular structure.

5. CONCLUSIONS

We analyzed high spatial resolution vertical slices of reflectivity and radial velocity through drizzling Sc in open and closed-cellular cloud regimes. In both regimes we observed drizzle growth from cloud top to cloud base and evaporation below cloud (Fig 3) as well as a tendency for convergence at low levels and divergence near cloud top, particularly in drizzle cell cores (Fig 4). The heights (relative to cloud top) and strengths of these divergence features were comparable between the two cloud regimes, which implies that the kinematic structure of the drizzle cells is also similar. The average cloud top height for the open-cellular clouds is somewhat lower, which may be partly caused by decreased entrainment resulting from a lower cloud fraction.

Individual RHIs provided evidence that the convergence and divergence patterns are occuring on the mesoscales. These results suggest that mesoscale variability within Sc drizzle can be parameterized in terms of the properties of sets of overturning convective cells of scale 2 to 20 km regardless of the cloud regime.

While the dynamics and microphysics of the drizzle cells were consistent between open and closed-cellular cloud regimes, the frequency distribution of drizzle cells varied somewhat. Strong drizzle cells occurred more frequently in the open-cellular regime (about 30% of the total number of cells, see Table 1) whereas closed-cellular regions contained more frequent moderate strength drizzle cells (about 90% of the total).

Drizzle potentially plays an important role in modulating the mesoscale circulations in Sc-topped boundary layers, affecting the cloud structure and radiative properties. It is important for cloud-resolving and other models to be able to reproduce the statistical features of drizzle cells presented here.

ACKNOWLEDGMENTS

The authors are grateful to Chris Fairall, Taneil Uttal, and Duane Hazen of NOAA ETL for providing MMCR data, and to the crew of the RHB for their assistance in data collection. This

research was funded by NSF grant ATM-0433712, NASA grant NNG04GA65G, and a NDSEG fellowship.

References

Agee, E. M., T. S. Chen, and K. E. Dowell, 1973: A review of mesoscale cellular convection. *Bull. Amer. Meteor. Soc.*, **54**, 1004–1012.

Bretherton, C. S., T. Uttal, C. W. Fairall, S. E. Yuter, R. A. Weller, D. Baumgardner, K. Comstock, and R. Wood, 2004: The EPIC 2001 stratocumulus study. *Bull. Amer. Meteor. Soc.*, **85**, 967–977.

Comstock, K., R. Wood, S. E. Yuter, and C. S. Bretherton, 2004: The relationship between reflectivity and rain rate in and below drizzling stratocumulus. *Q. J. R. Meteorol. Soc.*, **130**, 2891–2918.

Comstock, K. K., C. S. Bretherton, and S. E. Yuter, 2005: Mesoscale variability and drizzle in southeast Pacific stratocumulus, *J. Atmos. Sci.*, in press.

Moran, K. P., B. E. Martner, M. J. Post, R. A. Kropfli, D. C. Welsh, and K. B. Widener, 1998: An unattended cloud-profiling radar for use in climate research. *Bull. Amer. Meteor. Soc.*, **79**, 443–455.

Ryan, M., M. J. Post, B. Martner, J. Novak, and L. Davis, 2002: The NOAA Ron Brown's shipboard Doppler precipitation radar. *Proceedings of the 6th Symposium on Integrated Observing Systems*, Amer. Meteor. Soc., Orlando, FL.

Stevens, B., G. Vali, K. Comstock, R. Wood, M. C. vanZanten, P. H. Austin, C. S. Bretherton, and D. H. Lenschow, 2005: Pockets of open cells (POCs) and drizzle in marine stratocumulus. *Bull. Amer. Meteor. Soc.*, **86**, 51–57.

Wood, R. and D. Hartmann, 2005: Spatial variability of liquid water path in marine low cloud: Part II. Geographic distribution and dependence upon large-scale parameters, *J. Clim*, submitted.

Yuter, S. E. and K. K. Comstock, 2005: Satellite and radar characteristics of drizzling marine stratocumulus in the southeast Pacific, in preparation.

Yuter, S. E. and R. A. Houze, 1995: Three-dimensional kinematic and microphysical evolution of Florida cumulonimbus. Part II: Frequency distribution of vertical velocity, reflectivity, and differential reflectivity. *Mon. Wea. Rev.*, **123**, 1941–1963.